

# Strong increase of the electron effective mass in GaAs incorporating boron and indium

T. Hofmann<sup>#,1)</sup>, C. v. Middendorff<sup>1)</sup>, G. Leibiger<sup>2)</sup>, V. Gottschalch<sup>2)</sup>, and M. Schubert<sup>1)</sup>

HL 12.50

1) Institut für Experimentelle Physik II, Fakultät für Physik und Geowissenschaften, Universität Leipzig  
 2) Institut für Anorganische Chemie, Fakultät für Chemie und Mineralogie, Universität Leipzig

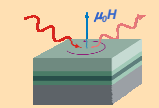
#E-mail: Tino.Hofmann@physik.uni-leipzig.de

## Our message

The novel low band-gap material BInGaAs shows obscure band structure properties:

- Strong increase of the  $\Gamma$ -point optical effective electron mass on incorporation of B and In
- Unexpected increase of the effective electron mass with decreasing free-charge-carrier concentration

### Fir MO-ellipsometry

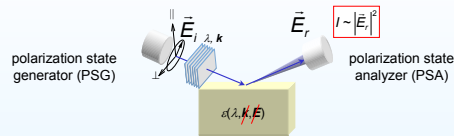


Non-contact, optical determination of the free-charge-carrier parameters concentration, effective mass, and mobility in layered structures:

see also Poster HL 12.90!

Contacts: NO!  
 Heterostructures: YES!

## Experimental setup



## Model-dielectric function

Polar lattice contribution

Electronic contribution    Infrared-active phonon modes    Alloy-induced modes    Free-carrier contribution

$$\epsilon_j(\omega, H) = \epsilon_{\infty,j} - \sum_{i=1}^l \frac{\omega^2 + i\gamma_{LO,i}\omega - \omega_{LO,i}^2}{\omega^2 + i\gamma_{TO,i}\omega - \omega_{TO,i}^2} \cdot \prod_{k=1}^m \left( 1 + \frac{i\delta\gamma_{kj} \omega - \delta\omega_{kj}^2}{\omega^2 + i\gamma_{AM,k} \omega - \omega_{AM,k}^2} \right) - \epsilon_j^{(FC-MO)}(\omega, H)$$

- ▶ Infrared-active phonon modes:  $\omega_{TO,LO}$  – TO/LO phonon mode frequency,  $\gamma_{TO,LO}$  – TO/LO broadening parameter
- ▶ alloy-induced modes:  $(\omega_{TO} - \omega_{LO}) \ll \omega_{TO}, \omega_{LO}$ ,  $\delta\omega_k = \omega_{LO,k}^2 - \omega_{TO,k}^2$ ,  $\gamma_{AM,k} = \gamma_{TO,k}$ , and  $\omega_{AM,k} = \omega_{LO,k}$

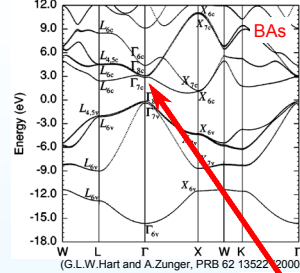
- ▶ Free-carrier contribution:  $\omega_{pl} \times \epsilon_j = (Nm_j^*)^{0.5}$  – plasma frequency,  $\gamma_{fc} \times \epsilon_j = (m_j^*)^{-1}$  – scattering tensor,  $N$  – free-carrier concentration,  $m_j^*$  – free-carrier effective mass tensor,  $\mu_j$  – free-carrier mobility tensor

$$\epsilon_j^{(FC-MO)}(\omega, H=0) = \frac{\omega_{pl}^2 \epsilon_{\infty,j}}{\omega(\omega + i\gamma_{fc,j})}$$

$\epsilon$  has tensor-character if  $H \neq 0!$

## BInGaAs – a new low band-gap material

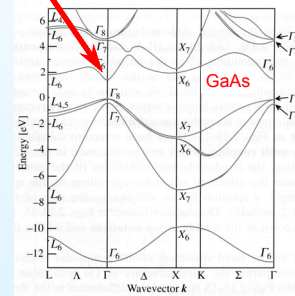
BInGaAs is a candidate for the 1eV band-gap absorber material in tandem solar cells with a widely unknown band structure!



Relativistic energy-band structure of BaAs (indirect). The lowest Brillouin-zone center conduction band of BaAs has  $\rho$  symmetry ( $\Gamma_{15c}$ , like Si) rather than  $s$  symmetry ( $\Gamma_{1c}$ , like GaAs or InAs).

first calculations indicate:

- small band-gap bowing in the BGaAs-alloy (compared to GaAsN)
- addition of B in GaAs and InGaAs increases the band-gap
- BGaAs behavior differs qualitatively from GaAsN



(P.Y.Yu and M. Cardona, Springer 1996)

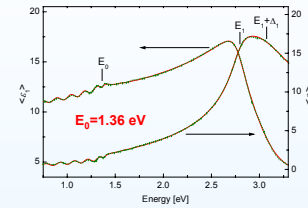
## Solar cell device

Design of a low band-gap solar cell based on BInGaAs as absorber material: see also Poster HL 44.55 on Thursday.

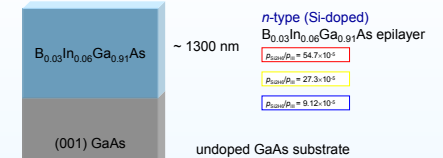
GaAs	Cap-layer	p-doped	$N = 5 \cdot 10^{18} \text{ cm}^{-3}$
GaNP	Window	p-doped	$N = 5 \cdot 10^{18} \text{ cm}^{-3}$
GaAs	Emitter	p-doped	$N = 1.5 \cdot 10^{18} \text{ cm}^{-3}$
BInGaAs	Base	n-doped	$N = 2 \cdot 10^{16} \text{ cm}^{-3}$
GaNP	Buffer	n-doped	$N = 1.1 \cdot 10^{17} \text{ cm}^{-3}$
GaAs	Buffer	n-doped	$N = 1.5 \cdot 10^{17} \text{ cm}^{-3}$
(001) GaAs	Substrate	n-doped	

## n-type BInGaAs with different Si concentrations

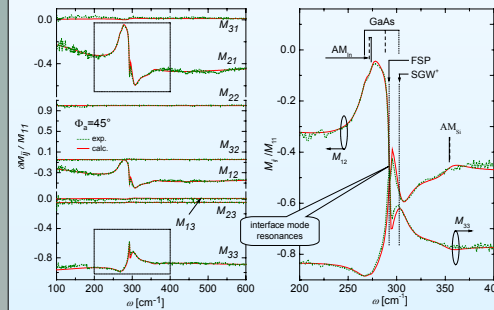
### NIR-VIS ellipsometry



Measured real  $\epsilon_1$  and imaginary  $\epsilon_2$  part of the pseudodielectric function of the sample with the highest Si-concentration. The solid lines represent the model analysis using the model dielectric function of Adachi.

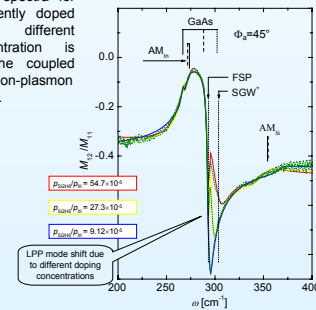


### Fir generalized ellipsometry

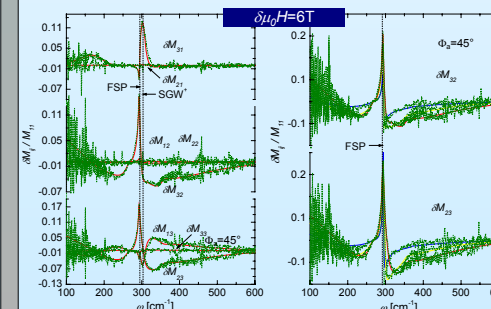


Comparison of the normalized  $M_{12}$  spectra for all three, differently doped samples. The different doping concentration is evident from the coupled longitudinal-phonon-plasmon mode (LPP) shift.

Mueller matrix elements normalized to  $M_{11}$ . Dominant structures originate from the GaAs-like Reststrahlen-band and the excitation of interface modes. The TO and LO phonon modes of the GaAs substrate can be recognized at  $\sim 268$  and  $\sim 292 \text{ cm}^{-1}$ .



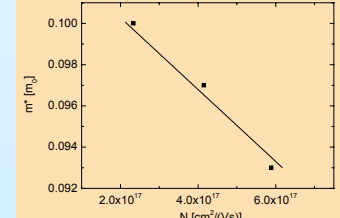
### Fir-mo generalized ellipsometry



The differences of the Mueller matrix elements measured at  $\mu_0 H = 3.0 \text{ T}$  and  $\mu_0 H = 6 \text{ T}$  represent the magnetic field induced changes of the ellipsometry data.

$m$ [m <sub>j</sub> ]	$N$ [10 <sup>17</sup> cm <sup>-3</sup> ]	$\mu$ [cm <sup>2</sup> (Vs)]
GaAs	0.067	
B <sub>0.037</sub> In <sub>0.06</sub> Ga <sub>0.902</sub> As:Si	0.093±0.003	5.9±0.3    888±22
	0.092±0.003	4.1±0.2    976±19
InAs	0.100±0.004	2.3±0.3    803±20
	0.023	

### First measurement of the effective electron mass in BInGaAs!



**New Data:**  
 - first measurement of  $m^*$  in B<sub>0.037</sub>In<sub>0.06</sub>Ga<sub>0.902</sub>As.  
 - strong increase of  $m^*$  compared to GaAs or InAs.  
 - unexpected  $m^*(N)$  behavior!